

Observing Topological Phase Transitions with High Harmonic Generation

Alexis Chacón^{1*}, Wei Zhu¹, Shane P. Kelly^{1,2}, Alexandre Dauphin³, Emilio Pisanty³, Antonio Picón^{3,4}, Christopher Ticknor¹, Marcelo F. Ciappina⁵, Avadh Saxena¹ and Maciej Lewenstein^{3,6}

¹Center for Non-linear Studies and Theoretical Division, Los Alamos National Laboratory, Los Alamos, New Mexico 87545, USA

²Physics and Astronomy Department, University of California Riverside, Riverside, California 92521, USA

³ICFO – Institut de Ciències Fotoniques, The Barcelona Institute of Science and Technology, 08860 Castelldefels (Barcelona), Spain

⁴Departamento de Química, Universidad Autónoma de Madrid, 28049 Madrid, Spain

⁵Institute of Physics of the ASCR, ELI-Beamlines project, Na Slovance 2, 182 21 Prague, Czech Republic

⁶ICREA, Pg. Lluís Companys 23, 08010 Barcelona, Spain

*alexis.chacon@lanl.gov

5 July 2018

Topological materials are of interest to both fundamental sciences and advanced technologies, because topological states are robust with respect to perturbations and dissipation, protected by topological invariants or underlying symmetries, i.e. time-reversal, inversion, particle-hole or other symmetries. Experimental detection of topological invariant is thus of great demand, but is extremely challenging. Ultrafast laser-matter interactions, leading to high harmonic generation (HHG) or laser-induced electron diffraction (LIED), were proposed several years ago to explore the structural and dynamical properties of various matter targets. Here, we show that HHG can be used to detect topological phases and phase transitions in the paradigmatic Haldane model. Analyzing intra- and inter-band currents via our theoretical approach, we find evidences to show that even and odd harmonics as well as their emitted intensities are sensitive to crossing a topological phase boundary. Our findings pave the way to understand fundamental questions regarding the complex ultrafast electron-hole pairs dynamics in topological materials by means of HHG.

The history of topological order goes back to the discovery of Integer and Fractional Quantum Hall Effects, awarded with Nobel prizes in 1985 [1] and 1998 [2], and the discovery of the Berezinsky-Kosterlitz-Thouless transition in 2D, awarded with Nobel prize in 2016 for topological concepts in Physics [3]. Topological order, due to its robustness and resistance to perturbations, has already found applications in standards and metrology (most notably, via the integer quantum Hall effect), and promises numerous applications from spintronics to quantum computing. Particularly interesting are possible applications of topological insulators (TI) [4] and superconductors [5].

Several methods have been proposed in the recent years, both in the context of real topological materials [6], and synthetic ones, employing ultracold atoms [7] and photonic systems [8, 9], among others. Nevertheless, new methods are still being sought for real materials. We here focus on the detection of topological phase transition and different topological phases by the non-linear optical responses of the medium in contrast to Ref. [8] where a linear response was suggested.

HHG was first proposed for the detection of molecular structure and orbitals in the seminal Ref. [10]. In HHG an ultrashort (5-15 fs) intense mid-infrared (MIR) laser pulse causes partial ionization of an electron in an atom/molecule.

The resulting electronic wave packet is accelerated in the laser-field, returns to the parent ion and recombines there, producing high-order harmonics [11, 12]. The efficiency of this process depends directly on the atomic/molecular orbital that the electron leaves and recombines with, and the electronic and molecular structure of the target can similarly be probed by the rescattered electron via laser-induced electron diffraction [13, 14].

In the last few years, the subject of HHG from solid-state targets has attracted considerable attention [15–17]. Generally, existing studies have dealt with standard materials, where the topology does not play a role and Berry-phase effects are not required, but more exotic systems have also been considered recently. In particular, Berry-phase effects have been explored in topologically-trivial materials, through experimental studies of HHG in atomically-thin semiconductors [18, 19], where the sensitivity of harmonic emission to symmetry breaking (specifically, the breaking of inversion symmetry in monolayer MoS₂ and α -quartz) is shown via the appearance of even harmonics and explained via semi-classical dynamics.

On more theoretical grounds, the effects of gap closing on the cutoff energy has been discussed by Zúrrón *et al.* [20] in graphene, where the first step in the HHG process initiated by the non-adiabatic crossing of the valence band electron trajectories through the Dirac points, instead of tunneling. Silva *et al.* [21] showed that HHG can be used to detect a dynamical Mott-insulator transition in strongly-correlated 1D solids. Bauer and Hansen [22] were the first to show that HHG is sensitive to topological order, by probing the contribution of edge states in a 1D chain analogous to the Su-Schrieffer-Heeger model [23], which they solved using time-dependent density functional theory.

In this letter, we push this idea to a natural culmination and demonstrate the possibility of using HHG for detection of topological invariants in 2D materials, such as the paradigmatic Haldane model, HM, [24], which we illustrate in Fig. 1. We derive and apply the theory of HHG in a two-band model solid, including fully the effects of the Berry connection and curvature. We characterize and analyze the HHG spectrum: the intra- and inter-band contributions, as well as harmonics with polarizations parallel and perpendicular to the driving laser, in the so called Keldysh approximation. Our theory is invariant with respect to the electromagnetic and Bloch gauges where the latter corresponds to multiplying

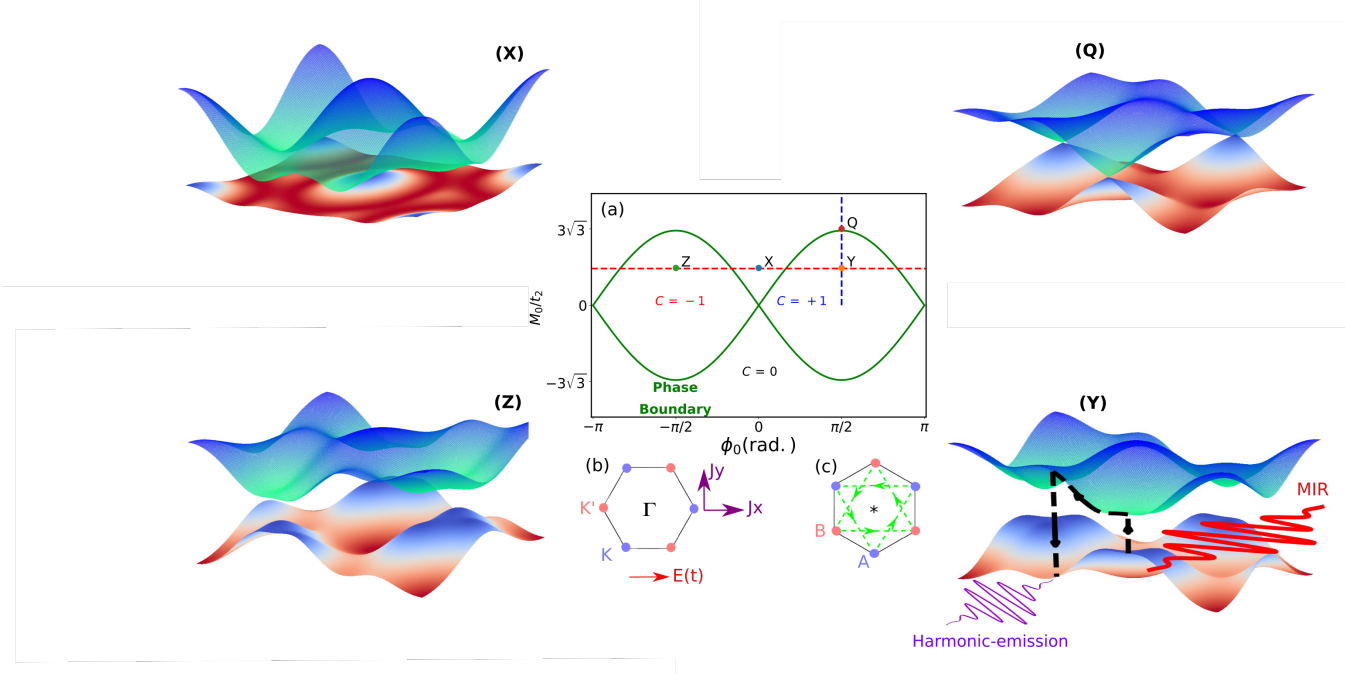


Figure 1 | Global phase diagram of Haldane model in the plane $(\phi_0, M_0/t_2)$, where different phases are distinguished by topological Chern number C . Phase boundary transition is depicted in green line of (a). Illustrations of the energy band-structure at representative points (X), (Y), (Z) and (Q) as shown in the phase-diagram (a). In particular, at the boundary (red-dot point label by Q), the band structure exhibits an interesting Dirac gapless point at K points but not at K' ones in the BZ. (Y) and (Z) depict the band-structure once the topological invariant are $C = \pm 1$ at the phase point $\phi_0 = \pm\pi/2$ and $M_0/t_2 = 2.54$. (Y) shows how the mid-infrared, MIR or laser-source oscillations (red-solid line) drives the topological material. We also depict a physical cartoon of the electron-hole pairs dynamics driven by the laser, i.e. creation, propagation and annihilation or recombination by the black-dashed lines with arrows, and finally the subsequent harmonic-emission (violet oscillations). The red-dashed horizontal and blue-dashed vertical lines in (a) point out, in addition, the phase-diagram region to which we shall investigate how the HHG spectrum behaves for the *topological-phase transition* and *difference topological invariants*. In (b) the momentum-space “lattice” as well as the laser-field linearly polarized stage along $\Gamma - K$ direction (horizontal red arrow) used in most of our calculations. The corresponding parallel and perpendicular current-emissions with respect to the fundamental laser-field are also in horizontal- J_x , and vertical-violet arrows, J_y , respectively. The panel (c) depicts our real-space honeycomb lattice with the atoms placed at A and B.

the Bloch functions of quasi-momentum \mathbf{k} with an arbitrary \mathbf{k} -dependent phase factor (See the Supplementary Material, SM). We perform a saddle point analysis, in which the semi-classical electron-hole pair trajectories include the phases of dipoles transition moments to assure the full gauge invariance (in contrast to Ref. [25]).

Our theory predicts the following: (i) HHG is extremely sensitive to inversion symmetry (IS) and, in addition, to the breaking time-reversal symmetry (TRS). (ii) The HHG spectrum and characteristics depend qualitatively on the topological phases, especially when both discrete symmetries are broken. (iii) We present a complete model, which captures the reported features of experiments [18, 19], and predicts novel behaviours for topologically non-trivial systems. (iv) We verify our theoretical approach by means of the exact density matrix time-dependent propagation.

In a semiconductor or insulator driven by mid-infrared lasers or THz sources, the harmonic emission is governed by the coherent sum of the intra-, $\mathbf{J}_{ra}(t)$, and inter-band, $\mathbf{J}_{er}(t)$, current oscillations, $\mathbf{J}(t) = \mathbf{J}_{ra}(t) + \mathbf{J}_{er}(t)$ [15, 16]. Those are

defined according to,

$$\mathbf{J}_{ra}(t) = \sum_m \int_{BZ} \mathbf{v}_m(\mathbf{K} + \mathbf{A}(t)) n_m(\mathbf{K}, t) d^3\mathbf{K}, \quad (1)$$

$$\mathbf{J}_{er}(t) = \frac{d}{dt} \int_{BZ} \mathbf{d}_{cv}^*(\mathbf{K} + \mathbf{A}(t)) \pi(\mathbf{K}, t) d^3\mathbf{K} + c.c. \quad (2)$$

where $\mathbf{v}_m(\mathbf{k}) = \mathbf{v}_{gr,m}(\mathbf{k}) + \mathbf{v}_{a,m}(\mathbf{k})$ is the m -th particle classical velocity. Here, m is an index which stands for the valence/conduction band, i.e. $m = v/c$. $\mathbf{v}_{gr,m}(\mathbf{k}) = \nabla_{\mathbf{k}} \varepsilon_m(\mathbf{k})$ is the particle, i.e. electron or hole, group velocity and $\mathbf{v}_{a,m}(\mathbf{k}) = \mathbf{E}(t) \times \boldsymbol{\Omega}_m(\mathbf{k})$, the anomalous velocity. $\varepsilon_m(\mathbf{k})$ is the energy dispersion band. \mathbf{K} denotes the quasi-canonical momentum defined in terms of the particle crystal momentum \mathbf{k} and the vector potential $\mathbf{A}(t)$ of the electric laser-field $\mathbf{E}(t) = -\partial_t \mathbf{A}(t)$ (for derivation see SM).

Note that, in experiments, it is possible to measure independently HHG emission with parallel (\parallel) and perpendicular (\perp) configurations with respect to the linear polarization of the driving laser [18, 19], which our theory does too (see laser and band structure scheme of Fig. 1). In addition, our theory allows us to treat inter- and intra- contributions separately and compare them.

We start by analyzing the recent HHG experiment of Luu *et*

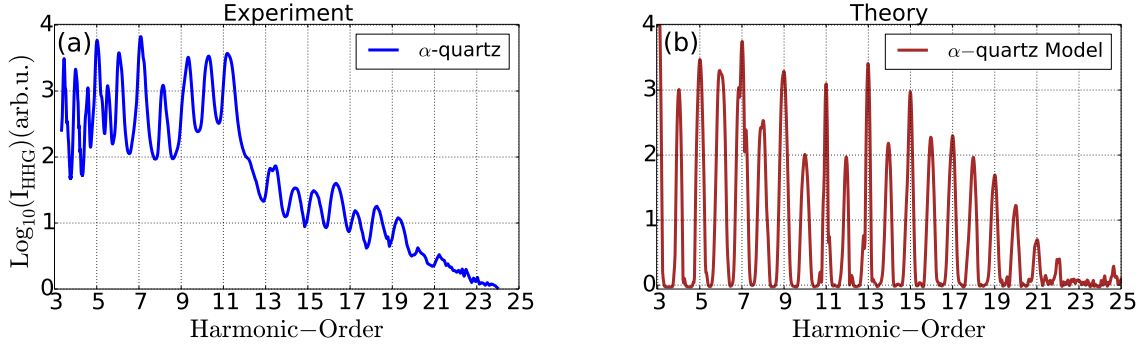


Figure 2 | High-order harmonic from trivial topological materials. (a) Experimental and (b) theoretical comparison of the HHG from α -quartz crystal, respectively. Both the theoretical and experimental data are averaged along parallel and perpendicular harmonic-emission with respect to fundamental polarization stage of the fundamental driven 800 nm laser. We employ similar laser features used on that experiment [19]. We normalize our HHG intensity calculations by multiplying a constant factor which matches the (HO, harmonic order) HO^{7th} of the experimental data.

al. [19] on α -quartz (SiO_2). Since a cut along z -direction of this crystal has an approximated honeycomb lattice structure, we use the trivial limit of HM to validate our theory (See SM). Due to the breaking of IS in α -quartz, the HHG spectrum contains even harmonics, shown in Fig. 2(a), mainly along the \perp emission configuration. Generally, the experimental features of [19] are well reproduced by our theory (see Fig. 2(b)); similar observations in MoSi_2 were reported in the seminal paper of Liu *et al.* [18], and we obtain good qualitative agreement with those results too. In our results, we observe that the intra-band contribution dominates for the lowest harmonic orders (HOs). On the other hand, the inter-band contribution dominates over the intra-band for high-order emitted photons. In the SM, we analyze these observations in more detail.

With this benchmark of our theory, we now turn to the Haldane model, a paradigmatic example of a Hamiltonian featuring topologically distinct phases of matter, exhibiting the anomalous quantum Hall effect and belonging to the class of Chern insulators. This model breaks both IS and TRS *without any net magnetic flux through the unit cell*, or better to say without Landau levels [24].

This model describes the hopping of electrons on a 2D hexagonal lattice with the standard nearest-neighbour hopping t_1 and a complex next-nearest-neighbour hopping $t_2 e^{i\phi_0}$, illustrated in Fig. 1, as well as an on-site potential offset M_0 . Here the TRS is broken via the phase ϕ_0 , which introduces a magnetic flux (see green arrows in Fig. 1(c)), and the IS is broken by the per-site potential M_0 , which controls the local potential difference between the two sub-lattices.

The phase diagram in the plane, $(\phi_0, M_0/t_2)$, shows three phases: a trivial phase where the topological invariant, the Chern number C , vanishes, shown as point X in Fig. 1, and two different topological phases at points Y and Z with $C = +1$ and -1 , respectively. The topological-phase boundaries are shown in green line of Fig. 1(a). We also show in Fig. 1 representative band structures for these different phases.

We now address the question whether HHG is an observable sensitive to topological-phase transitions and different topological phases. To this aim, we fix the ratio $M_0/t_2 = 2.54$ while varying the phase ϕ_0 of the next-nearest-neighbour “spin-orbit” coupling. In addition, we fix the nearest-neighbour coupling t_1 constant in such a way that

band-gap energy E_g changes between 0 and 4 eV (See Fig. 3) – a large range of energies close to experimental bandgap values of TIs. We show our key results in Fig. 3, for both \parallel and \perp emission configurations, and these display multiple interesting features.

First, variations in ϕ_0 , and with it in the topological invariant C , produce dramatic modifications of the harmonic signal. For instance, for $\phi_0 \neq 0$, IS and TRS are broken, even and odd harmonics arise for both \parallel and \perp emissions. Still, odd harmonics are clearly dominating in the $C = 0$ phase. Second, the inter-band contributions exhibit larger intensities than intra-band for high-harmonic orders; in contrast, the intra current dominates over the inter one for low harmonics, i.e. less than HO^{5th}. Note also that the parallel emission has a larger intensity than the perpendicular one. Third, the harmonic emissions for $\phi_0 = \pm\pi, 0$, are contains exclusively odd harmonics along the \parallel configuration, as well as the \perp component; this observation is in very good agreement with the calculations of α -quartz and the corresponding experimental measurements of [18, 19].

The large enhancement effect in harmonic intensity yield at the phase transition is associated to the Dirac point, at which the band-gap closes, which occurs at the topological-phases boundaries. However, this enhancement is not the only modification on the spectrum – even and odd harmonics arise “simultaneously” once C reaches ± 1 , and both symmetries TRS and IS are broken. This is more evident at the boundary of the phase transition.

These results show how the HHG spectrum is extremely sensitive to symmetry breaking (see SM for further details) and topological-phase transitions, as well as the band-gap closures at the transitions themselves.

In order to shed light on the origin of the different HHG spectra, we investigate two additional scenarios. In the first one, (i) the magnetic flux is fixed to $\phi_0 = \pi/2$ while the ratio M_0/t_2 varies from 0 to 10, and the topological invariant changes from $C = +1$ to 0. This provides a separate way of probing the topological phase transition at $M_0/t_2 \approx M_c = 3\sqrt{3}$ and, since the spectrum is very sensitive to the boundaries of the phases, we analyze a region far from the topological transition, $M_0/t_2 > M_c$. In the second scenario, (ii) the topo-

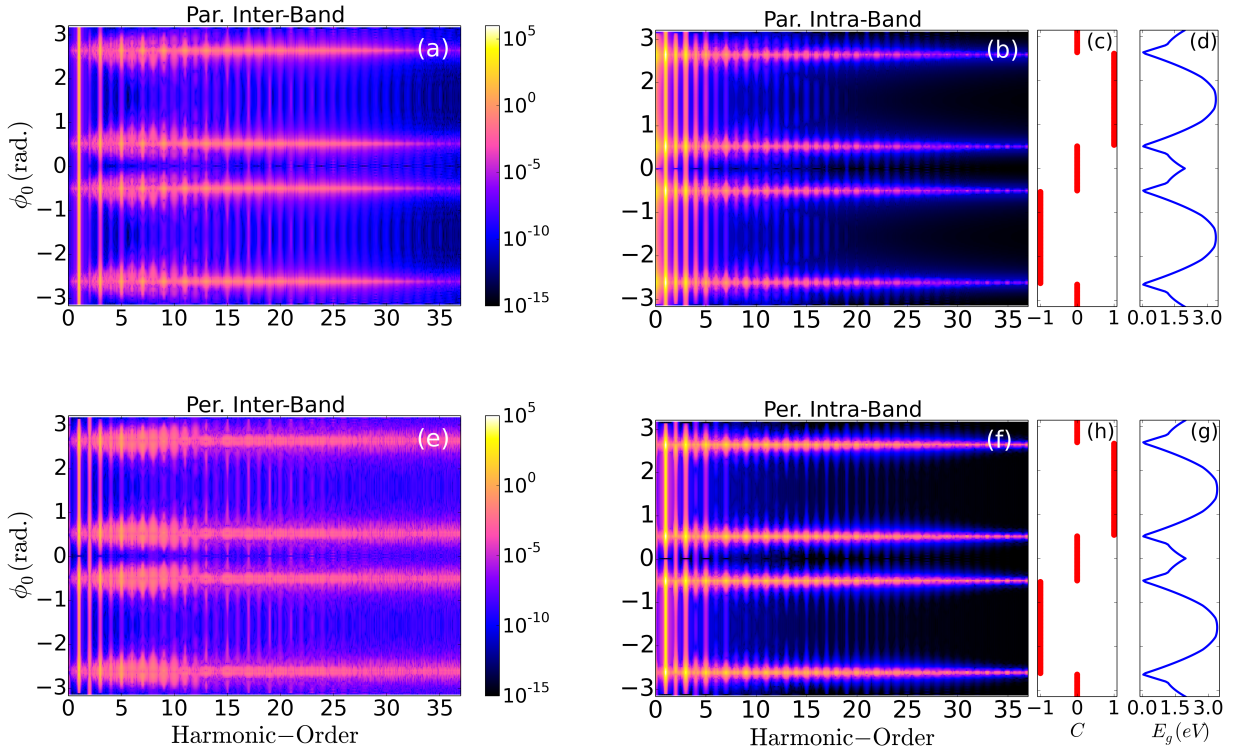


Figure 3 | Detection of topological-phase transition with HHG. Harmonic spectrum as a function of the magnetic flux ϕ_0 for parallel (a,b) and perpendicular (e,f) emissions with respect to the fundamental polarization mid-infrared laser, MIR. The inter-band (a,e) and intra-band (b,f) currents are considered. In last the right panels, (c,h), we have the Chern number, C , in red “circles” as well as the band-gap E_g (d,g) in blue-lines. We use a MIR laser-field linearly polarized along Γ – K crystal orientation, as it is depicted in Fig. 1b). We fixed the local potential to $M_0 = 0.0635$ a.u. (1.727 eV), $t_1 = 0.075$ a.u. (2.04 eV), $t_2 = t_1/3$ and the lattice constant $a_0 = 1.0 \text{ \AA}$, the laser-field wavelength is $3.25 \mu\text{m}$ ($\omega_0 = 0.014$ a.u.), with a time duration of 8 cycles at FWHM and a peak electric-field strength of $E_0 = 0.003$ a.u. ($I_0 = 3.5 \times 10^{11} \text{ W/cm}^2$).

logical invariant is $C = 0$ such that both TRS and IS break, i.e. a horizontal cut about $M_0/t_2 \sim 10$ in Fig. 1a). This leads to a magnetic flux region, where the HHG spectra are computed far from the boundary of phase transition, i.e. $|M_0/t_2| > 3\sqrt{3}$.

Since the \parallel emission intensity dominates over the \perp one, for the above two scenarios we show only the \parallel component of the combined contributions of both intra- and inter-band currents, in Fig. 4. In case of (i), (See Figs. 4(a)-(c)), we observe that once the local potential ratio M_0/t_2 increases, the harmonic-spectrum exhibits a structure of even and odd orders. This is noticed along the region of $C = +1$. Similarly to Fig. 3, enhancements of the harmonic signal with both even and odd harmonics are shown roughly at the band-gap closure at $M_0/t_2 = M_c$. Once the topological invariant changes to $C = 0$, even and odd harmonics are still observed about $M_0/t_2 \sim M_c$. This is attributed to the fact that HHG is extremely sensitive to the *topological-phase transition*. However, once $M_0/t_2 > M_c$, the odd harmonics dominate over evens for the highest orders, HO > 5th. In other words, the even harmonics are suppressed for the highest HOs as we find in Fig. 4(d). Hence, once the TRS and IS are broken, the above observation suggests that the *HHG spectrum* is indeed sensitive to *topological-phase transition* and the *variations on the Chern number*. The second scenario is illustrated in Figs. 4(e)-(g). When $M_0/t_2 \sim 10$ is larger than M_c and ϕ_0 varies, odd harmonics dominate over evens one for highest HOs.

To understand better the HHG sensitivity to topological phase transitions, we perform *quasi-classical saddle point analysis* and calculated relevant electron-hole pair trajectories for high HOs. These trajectories are sensitive to the topological features, such as the Berry curvature, the phase of dipole matrix elements and energy-band structure deformation, that take place at the excitation-recombination process (see Figs. 4(h)). This recombination picture is more evident for the inter-band contribution [16]. In the saddle-point analysis (i) electron-hole pairs are created by the driven field at the excitation time t' ; (ii) electron-hole pairs are accelerated along the parallel and perpendicular directions with respect to the driven laser-field between t' and t , birth and recombination times; electron-hole pairs can recombine or annihilate at time t with the subsequent photon energy emission. Finally, in Figs. 4(h), one observes how these classical trajectories depend on the Chern number.

In summary, our theory suggests that the HHG spectrum can be used to probe: (1) *topological-phase transitions*; (2) *topological invariants*; and (3) that it is *extremely sensitive to symmetry breaking of time-reversal and inversion*. Those are important results, since (i) our theory can be applied to a larger range of topological materials with similar band-gap properties described in this manuscript and extended to THZ sources [26]. Another possible application could be Bi_2Se_3 , which is a good candidate for topological insulator; possible layers thick modifications could be created in this material in

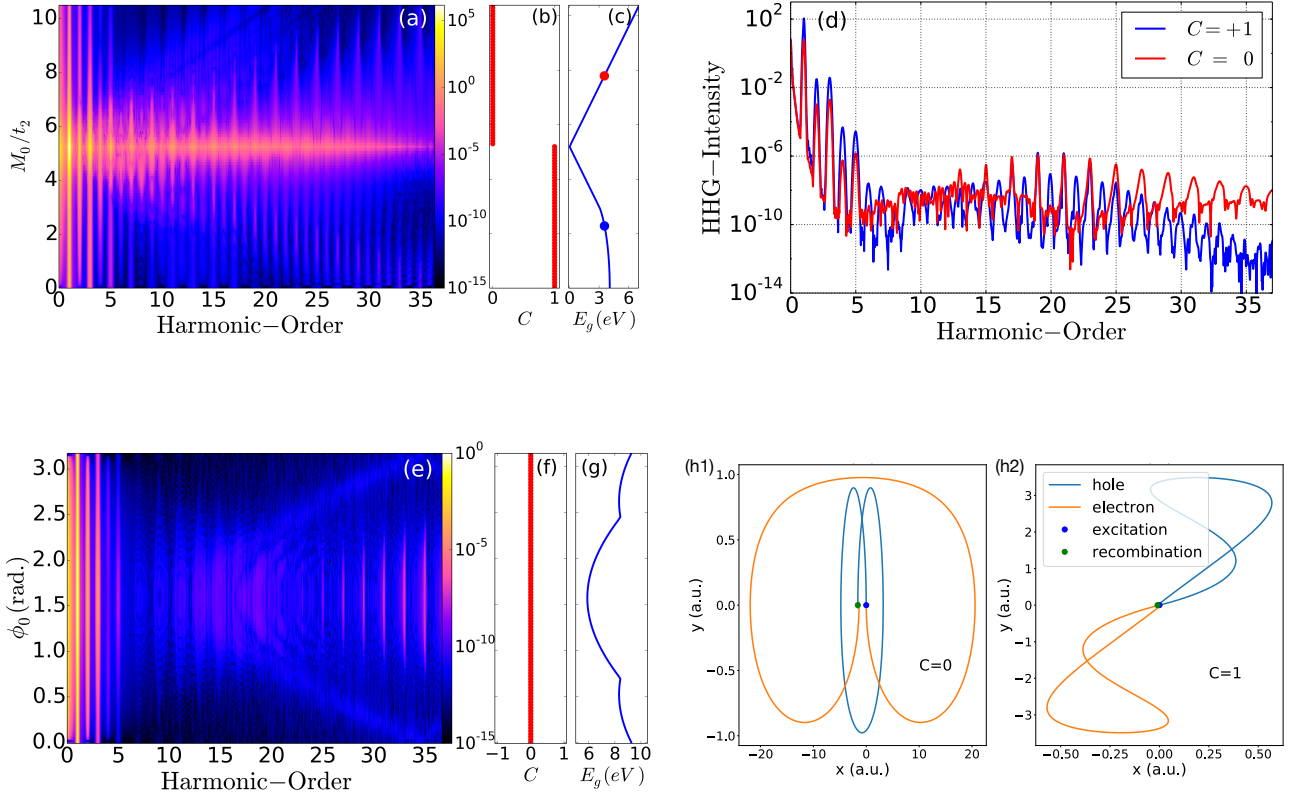


Figure 4 | Harmonic emission around and “far” from the topological-phase boundary transition. (a), (b) and (c) show the full (inter-band + intra-band) parallel HHG emission, the topological invariant $C = +1$ and 0 and the band-gap energy as a function of the M_0/t_2 . (d) Harmonic spectrum for two different phases $C = +1$ and 0 for the same band-gap, $E_g = 3.5$ eV while the magnetic flux is fixed at $\phi_0 = \pi/2$ (see blue and red dots of (c)). (e), (f) and (g) depict the HHG spectrum similar than in (a), but as a function of the flux ϕ_0 once the ratio $M_0/t_2 \sim 10 > M_c$ is fixed, Chern number C and band-gap energies E_g vs ϕ_0 , respectively. Here, $M_c = +3\sqrt{3}$ is the critical ratio M_0/t_2 to which the topological-phase transition takes place at $\phi_0 = \frac{\pi}{2}$. Last panel (h) depicts classical electron-hole trajectories for $C = 0$ (h1) and $C = +1$ (h2) with their corresponding creation (blue-dot) – annihilation (green-dot) positions which eventually leads to the high-photon emission. Laser parameters are the same than in Fig. (3).

order to control the topological transition as in Ref. [27], (ii) Terahertz sources open a path to access to the HHG in topological materials with the photon-energy less than the band-gap in two different topological orders, (iii) this opens also new questions about exploring the dynamics in the strongly correlated systems with spin-orbit couplings; (iv) the emission control of even and odd harmonics would lead to manipulate the time-delay between the generated outcome pulses; this is extremely important for the studies of ultrafast electronic dynamics in molecules and solids via pump-probe experiments.

Methods

The derivation of the semiconductor Bloch equations and time dependent density matrix propagation that describe the laser-crystal interactions in a topological solid material is presented in the supplementary material. We discuss there also the details of derivation of gauge invariant saddle point equations describing quasi-classical electron-hole trajectories.

Acknowledgements

We thank T. T. Luu and H. J. Wörner for providing us the experimental data in editable format. We acknowledge the Spanish Ministry MINECO (National Plan 15 Grant: FISICATEAMO No. FIS2016-79508-P, SEVERO OCHOA No. SEV-2015-0522, FPI), European Social Fund, Fundació

Cellex, Generalitat de Catalunya (AGAUR Grant No. 2017 SGR 1341 and CERCA/Program), ERC AdG OSYRIS, EU FETPRO QUIC, and the National Science Centre, Poland-Symfonia Grant No. 2016/20/W/ST4/00314. A.P. acknowledges funding from Comunidad de Madrid through TALENTO grant ref. 2017-T1/IND-5432. M.F.C. thanks support of the project Advanced research using high intensity laser produced photons and particles (CZ.02.1.01/0.0/0.0/16 019/0000789) from European Regional Development Fund (ADONIS).

The authors gratefully acknowledge support from the Science Campaigns, Advanced Simulation, and Computing and LANL, which is operated by LANS, LLC for the NNSA of the U.S. DOE under Contract No. DE-AC52-06NA25396 and the Center of Nonlinear Studies of LANL. S. K. acknowledges financial support from the UC Office of the President through the UC Laboratory Fees Research Program, Award Number LGF-17- 476883.

At the final stage of preparation of this manuscript, we became aware of a parallel work at [arXiv:1806.11232](https://arxiv.org/abs/1806.11232).

References

- [1] K. von Klitzing. The quantized Hall effect. *Rev. Mod. Phys.* **58** no. 3, pp. 519–531 (1986); Nobel Prize lecture.

- [2] H. L. Stormer. Nobel lecture: The fractional quantum Hall effect. *Rev. Mod. Phys.* **71** no. 4, pp. 875–889 (1999); Nobel Prize lecture. R. B. Laughlin. Nobel lecture: Fractional quantization. *Rev. Mod. Phys.* **71** no. 4, pp. 863–874 (1999); Nobel Prize lecture. D. C. Tsui. Nobel lecture: Interplay of disorder and interaction in two-dimensional electron gas in intense magnetic fields. *Rev. Mod. Phys.* **71** no. 4, pp. 891–895 (1999); Nobel Prize lecture.
- [3] J. M. Kosterlitz. Nobel lecture: Topological defects and phase transitions. *Rev. Mod. Phys.* **89** no. 4, p. 040 501 (2017); Nobel Prize lecture. F. D. M. Haldane. Nobel lecture: Topological quantum matter. *Rev. Mod. Phys.* **89** no. 4, p. 040 502 (2017); Nobel Prize lecture.
- [4] X.-L. Qi and S.-C. Zhang. Topological insulators and superconductors. *Rev. Mod. Phys.* **83** no. 4, pp. 1057–1110 (2011). arXiv:1008.2026.
- [5] C. Nayak, S. H. Simon, A. Stern, M. Freedman and S. Das Sarma. Non-abelian anyons and topological quantum computation. *Rev. Mod. Phys.* **80** no. 3, pp. 1083–1159 (2008). arXiv:0707.1889.
- [6] M. Z. Hasan and C. L. Kane. Colloquium: Topological insulators. *Rev. Mod. Phys.* **82**, pp. 3045–3067 (2010). arXiv:1002.3895.
- [7] N. Goldman, G. Juzeliunas, P. Öhberg and I. B. Spielman. Light-induced gauge fields for ultracold atoms. *Rep. Prog. Phys.* **77** no. 12, p. 126 401 (2014). arXiv:1308.6533.
- [8] W. J. M. Kort-Kamp. Topological phase transitions in the photonic spin Hall effect. *Phys. Rev. Lett.* **119**, p. 147 401 (2017). arXiv:1707.02057.
- [9] T. Ozawa, H. M. Price, A. Amo, N. Goldman, M. Hafezi, L. Lu, M. Rechtsman, D. Schuster, J. Simon, O. Zilberberg and I. Carusotto. Topological photonics. arXiv: 1802.04173.
- [10] J. Itatani, J. Levesque, D. Zeidler, H. Niikura, H. Pépin, J.-C. Kieffer, P. B. Corkum and D. M. Villeneuve. Tomographic imaging of molecular orbitals. *Nature* **432** no. 432, pp. 867–871 (2004).
- [11] P. B. Corkum. Plasma perspective on strong field multi-photon ionization. *Phys. Rev. Lett.* **71**, p. 1994 (1993).
- [12] M. Lewenstein, P. Balcou, M. Y. Ivanov, A. L’Huillier and P. B. Corkum. Theory of high-harmonic generation by low-frequency laser fields. *Phys. Rev. A* **49**, p. 2117 (1994).
- [13] T. Zuo, A. D. Bandrauk and P. B. Corkum. Laser-induced electron diffraction: a new tool for probing ultrafast molecular dynamics. *Chem. Phys. Lett.* **259**, p. 313 (1996). HAL eprint.
- [14] B. Wolter, M. G. Pullen, A. T. Le, M. Baudisch, K. Doblhoff-Dier, A. Senftleben, M. Hemmer, C. D. Schröter, J. Ullrich, T. Pfeifer, R. Moshammer, S. Gräfe, O. Vendrell, C. D. Lin and J. Biegert. Ultrafast electron diffraction imaging of bond breaking in di-ionized acetylene. *Science* **354**, pp. 308–312 (2016). UPCommons eprint.
- [15] S. Ghimire, A. D. DiChiara, E. Sistrunk, P. Agostini, L. F. DiMauro and D. A. Reis. Observation of high-order harmonic generation in a bulk crystal. *Nat. Phys.* **7** no. 2, pp. 138–141 (2011). OSU eprint.
- [16] G. Vampa and T. Brabec. Merge of high harmonic generation from gases and solids and its implications for attosecond science. *J. Phys. B: At. Mol. Opt. Phys.* **50** no. 8, p. 083 001 (2017).
- [17] E. N. Osika, A. Chacón, L. Ortmann, N. Suárez, J. A. Pérez-Hernández, B. Szafran, M. F. Ciappina, F. Sols, A. S. Landsman and M. Lewenstein. Wannier-bloch approach to localization in high-harmonics generation in solids. *Phys. Rev. X* **7** no. 2, p. 021 017 (2017).
- [18] H. Liu, Y. Li, Y. S. You, S. Ghimire, T. F. Heinz and D. A. Reis. High-harmonic generation from an atomically thin semiconductor. *Nat. Phys.* **13** no. 3, p. 262 (2017). Stanford eprint.
- [19] T. T. Luu and H. J. Wörner. Measurement of the Berry curvature of solids using high-harmonic spectroscopy. *Nat. Commun.* **9** no. 1, p. 916 (2018).
- [20] O. Zurrón, A. Picón and L. Plaja. Theory of high-order harmonic generation for gapless graphene. *New J. Phys.* **20** no. 20, p. 053 033 (2018).
- [21] R. E. F. Silva, I. V. Blinov, A. N. Rubtsov, O. Smirnova and M. Ivanov. High-harmonic spectroscopy of ultrafast many- body dynamics in strongly correlated systems. *Nat. Phot.* **12** no. 2, pp. 266–270 (2018). arXiv:1704.08471.
- [22] D. Bauer and K. K. Hansen. High-harmonic generation in solids with and without topological edge states. *Phys. Rev. Lett.* **120** no. 6, p. 177 401 (2018). arXiv:1711.05783.
- [23] W. Su, J. Schrieffer and A. J. Heeger. Solitons in polyacetylene. *Phys. Rev. Lett.* **42**, p. 1698 (1979).
- [24] F. D. M. Haldane. Model for a quantum Hall effect without Landau levels: Condensed-matter realization of the “parity anomaly”. *Phys. Rev. Lett.* **61** no. 18, pp. 2015–2018 (1988).
- [25] F. Yang and R.-B. Liu. Berry phases of quantum trajectories of optically excited electron-hole pairs in semiconductors under strong terahertz fields. *New J. Phys.* **15** no. 11, p. 115 005 (2013). arXiv:1211.3021.
- [26] P. Rodriguez-Lopez, W. J. M. Kort-Kamp, D. A. R. Dalvit and L. M. Woods. Nonlocal optical response in topological phase transitions in the graphene family. *Phys. Rev. Materials* **2**, p. 014 003 (2018). arXiv:1711.06311.
- [27] M. Neupane et al. Observation of quantum-tunnelling-modulated spin texture in ultrathin topological insulator bi₂se₃ films. *Nature Comm.* **5** no. 3841, pp. 1–7 (2014). arXiv:1404.2830.